Int. J. Heat Mass Transfer. Vol. 35, No. 9, pp. 2245–2256, 1992
Printed in Great Britain

0017–9310/92 $5.00 + 0.00

Benard convection in a two-component system with Soret effect

G. ZIMMERMANN† and U. MÜLLER
Kernforschungszentrum Karlsruhe GmbH, Institut für Reaktorbauelemente, Postfach 3640, 7500 Karlsruhe 1, F.R.G.

(*Received* 15 *May* 1991)

Abstract—The spatial and temporal behaviour of Rayleigh–Benard convection in a two component system with Soret effect is studied by employing differential interferometry in combination with local temperature records inside the liquid layer. Travelling roll patterns of transient and permanent character as well as steady overturning convection are observed. The frequencies associated with the travelling waves are determined and compared with predictions of linear stability analysis and interpreted in terms of solute transport and mixing along streamlines. An unexpected feature is that the range of occurrence of the permanent state of travelling waves shrinks when non-Boussinesq effects dominate.

1. INTRODUCTION

A BINARY liquid mixture subject to temperature gradients generates thermal diffusion, i.e. temperature gradients cause solute fluxes. This phenomenon is known as the Soret effect. The induced Soret solute flux may either add to or subtract from the imposed thermal gradient. In the latter case the opposing fields may generate oscillatory convective responses.

Convection in binary mixtures with negative Soret coefficient has been investigated intensively in the past two decades. Caldwell [1] studies Benard convection in salt-water while Hurle and Jakeman [2] and Platten and Chavepeyer [3] perform experiments in alcohol–water mixtures. They describe stable permanent states of oscillatory convection of constant frequency. Alcohol–water mixtures have proven particularly easy to handle and have been utilized by numerous investigators (Walden *et al.* [4], Kolodner *et al.* [5, 6], Surko and Kolodner [7], Moses and Steinberg [8], Steinberg *et al.* [9], Ahlers *et al.* [10], Fineberg *et al.* [11, 12], Bensimon *et al.* [13]) in their studies of the dynamics of convection in mixtures with Soret effects. In many of these recent experiments a light-scattering method has been employed in order to visualize the time dependent behaviour of the convection cell pattern. The convection pattern is visualized from above through a transparent upper boundary of the test cell by generating shadowgraphs of the light reflected from the mirror polished bottom of the test cell. The main results from these experiments can be summarized as follows:

(a) Immediately after the onset of a weak convection for slightly supercritical temperature differences across the layer, the roll pattern starts moving in the horizontal direction perpendicular to the roll axis. The convection presents itself as a travelling wave with modulation of the amplitudes.

(b) The low intensity state of travelling waves is unstable with regard to a stable, permanent state of travelling waves characterized by a constant phase velocity.

(c) If the temperature difference across the layer is increased, the phase velocity of the stable state of travelling wave decreases and ends up in a smooth transition to steady convection, often called overturning convection.

The stability of the static state of a binary mixture with Soret effect was studied theoretically by Hurle and Jakeman [2], Schechter *et al.* [14] and Legros *et al.* [15]. Chock and Li [16] and Zimmermann [17] solve the linear stability problem for a complete set of balance equations, describing the transport processes in mixtures. The essential results of the linear stability analysis can be summarized in terms of the Soret number S as a measure for the intensity of thermal mass. There is a critical value S^* of S such that $S^* < 0$. There are two cases that occur when the temperature difference across the layer exceeds a critical value. When $S > S^*$, the static state is replaced by a state of steady convection. When $S < S^*$, a state of oscillatory convection occurs. At $S = S^*$ both convective states merge at a codimension-two point. In Fig. 1 calculated values of the critical Rayleigh numbers, wave numbers and oscillation frequencies for a typical binary mixture S are shown as a function of the Soret number.

Weakly nonlinear theories for finite amplitude convection in binary mixtures have recently been developed by Knobloch [18] and Cross [19]. Although these authors assume stress free and solute permeable boundaries in their model equations they do predict travelling wave states. Linz *et al.* [20] have improved an 8-mode Galerkin model by taking into account realistic boundary conditions for the solute, i.e. vanishing solute flux at the boundaries.

† Present address: Aachen Center for Solidification in Space e.V., Intzestraße 5, W-5100 Aachen, F.R.G.

NOMENCLATURE

a	constant
C	concentration [wt fr.]
D	molecular diffusivity [$m^2 s^{-1}$]
e	beam splitting [m]
f	frequency [Hz]
g	gravity vector [$m^2 s^{-1}$]
h	cell height [m]
j	mass flux [$m s^{-1}$]
k	wave number [dimensionless]
L	length [m]
n	vertical unit vector
Pe	Peclet number
R	Rayleigh number
r	reduced Rayleigh number
S	Soret number
So	Soret coefficient [K^{-1}]
s	path [m]
T	temperature [K]
t	time [s]
U	transport velocity [$m s^{-1}$]
u, v, w	velocity components [$m s^{-1}$]
V	front velocity [$m s^{-1}$]
v	velocity vector.

Greek symbols

α	thermal expansion coefficient [K^{-1}]
α'	solution expansion coefficient [(wt fr.)$^{-1}$]
δ	variation
Δ	difference
κ	thermometric conductivity [$m^2 s^{-1}$]
ν	kinematic viscosity [$m^2 s^{-1}$]
ρ	density [$kg m^{-3}$]
τ	period time [s]
ω	frequency [dimensionless].

Superscripts

(o)	oscillatory
(s)	stationary
*	critical.

Subscripts

o	lower boundary
1	upper boundary
0	mean value
c	critical value
D	solutal
T	thermal
t	turn around
mix	mixing.

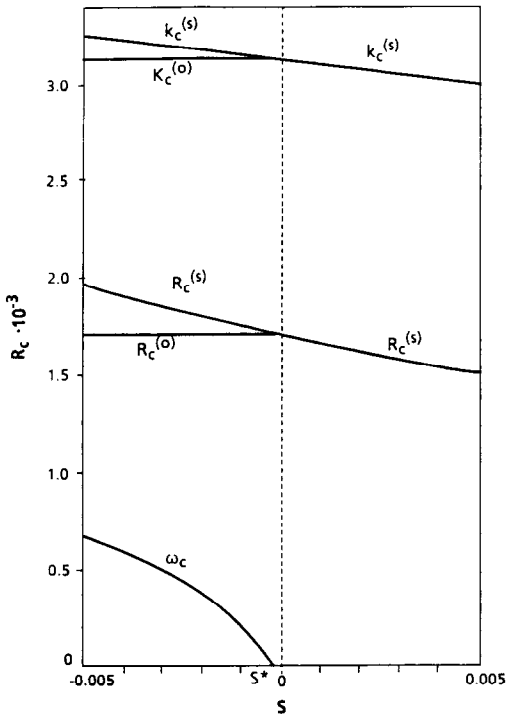

FIG. 1. Critical Rayleigh number R_c, critical wave number k_c, critical angular frequency ω_c as a function of the Soret number S for an initial concentration $C_0 = 0.01$. S^* denotes a codimension-two point.

In spite of the encouraging results obtained by the cited authors and others from nonlinear analysis, many of the experimentally-observed phenomena cannot be explained sufficiently well today. Some technically interesting aspects of convection in binary mixtures, such as influence of temperature dependent physical properties of the mixture, and the nonlinear density–temperature relationship, have not been investigated up to this date. The experimental investigations reported in this article will support the findings of previous authors by employing different visualization and measuring techniques and, moreover, will address the effect of a nonlinear density–temperature relationship on the oscillatory convection.

2. EXPERIMENTS

2.1. *Experimental techniques*

The experiments are performed in a rectangular test volume of aspect ratio length : width : height = 200 mm : 20 mm : 3.12 mm in order to foster the generation of regular roll convection patterns (Fig. 2). The volume is demarked by two copper blocks which serve as the upper and lower boundaries. Crystal glass plates form the long side walls. Two Teflon blocks are placed between the copper blocks and simultaneously serve as spacer elements and shorter side walls. O-rings are employed to seal off the cavity. The

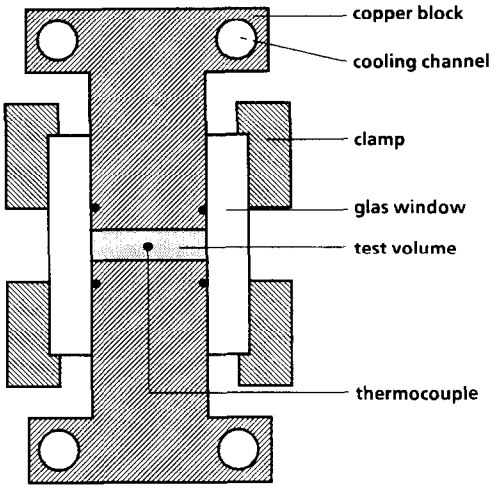

FIG. 2. Cross-section of the test apparatus.

copper blocks are heated or cooled by circulating temperature-controlled coolant from thermostats through jackets at the upper and lower end of the two blocks. The overall design of the test apparatus is based on three-dimensional heat-conduction calculations that provide a very good approximation to a linear temperature distribution across the cavity in the preconvective state. According to calculations, horizontal-temperature inhomogeneities are less than 0.1% at the ends of the longsides and less than 0.01% otherwise. Nearly-ideal temperature conditions before onset of convection are needed to investigate the transition to oscillatory flow, since even the smallest convective motions, due to temperature inhomogeneities, may disturb significantly the concentration profile in the layer. The test apparatus is insulated externally by a styrofoam cover and, further, is placed in an air-conditioned chamber with good temperature control. The air temperature in this chamber is kept at the mean temperature of the test liquid during the experiments, i.e. $\bar{T} = \frac{1}{2}(T_1 + T_0)$. This procedure proved to be necessary for tests with solidification at temperatures significantly lower than the laboratory temperature which will be reported in a succeeding paper.

The selection of a suitable test liquid is crucial for a clear experimental identification of the phenomena. For our experiments we choose as a test liquid ethyl alcohol–water mixtures. The physical properties of this mixture are well documented in the literature. In particular the Soret number S which characterizes the thermal diffusion effect, can be varied between negative and positive values by changing the concentration of the solute and the mean temperature in the test liquid (see ref. [21]). Mixtures of 8 and 15 wt% ethyl alcohol and water are used in the experiments.

The quality of the measurement is determined by the long-term constancy of the temperatures at the upper and the lower boundary of the test cavity. These temperatures are controlled by two high-precision Haake thermostats of a coolant outlet-temperature-variance $\Delta T = \pm 0.01$°C. At low temperatures ethyl alcohol is used as a coolant. The thermostats are connected to the test apparatus by plastic hoses isolated by thick rubber-foam wrappings.

The flow in the cooling channels of the test apparatus is counter current. The temperature in the copper blocks are measured by precision platinum resistance thermometers which are threaded through bore holes in the copper blocks very close to the boundaries of the liquid layer. The measuring arrangement used determines the temperature difference across the layer to an accuracy of $\Delta T = \pm 0.002$ K. The quality of the temperature control of the test apparatus may be judged by the fact that for static or for stable flow conditions in the liquid layer the measured temperature difference is constant up to $\delta(\Delta T) = \pm 0.003$ K over time intervals of several days.

The temperature fluctuations within the liquid layer are measured by two NiCr–Ni thermocouples 0.25 mm in diameter protruding 0.9 mm into the test volume from the lower copper boundary. The thermocouple is located at the centre of this boundary. The voltage between this thermocouple and a reference thermocouple in the lower copper is recorded. This voltage is amplified and further processed to give signals of the temperature oscillations T' in the test liquid as a pen chart record. The resolution of the temperature oscillations is $\delta T' = \pm 0.02$ K for the measuring arrangement used. From the chart records the period τ of periodic temperature fluctuation can be evaluated by averaging over a sequence of 20 periods to an accuracy of $\delta\tau/\tau \simeq 0.01$.

The convective flow in the test volume was visualized by employing a differential interferometer (see ref. [22] for an outline of the technique). In general the differential interferometer generates lines of constant density differences in the direction of the beam separation. If the separation length e is small, as in the present case ($e = 0.3$ mm), lines of constant density differences become lines of constant temperature gradients. Since the inteferometer beams integrate the density differences only in one direction through the test volume, as is the case in the present set up, a quantitative evaluation of the fringe pattern is only possible for a perfectly two-dimensional flow. In the present experiment only horizontal beam splitting is used. Bühler *et al.* [22] has shown, for slightly supercritical conditions and two-dimensional flow, that the fringe pattern generated from horizontal beam splitting can be interpreted to a good approximation as the stream line pattern. The interferograms are recorded by a high resolution video camera. Further processing is performed by employing a digital image processing system. Each interferogram shown in the figures of Section 2.2 shows a 43 mm length of the total 200 mm length of the test volume. In order to take interferograms from each part of the test volume the interferometer is placed on an optical bench which can be moved transversely in a controlled manner. When there are moving cellular patterns, quantitative

determination of the wavelength and the direction and speed of the pattern movement can be easily made if one examines interferograms taken on-line or at distinct time intervals.

2.2. *Experimental results*

2.2.1. *Small amplitude initial perturbation.* Experiments are conducted in a liquid mixture of 15 wt% ethyl alcohol in water at different mean temperatures $\bar{T} = \frac{1}{2}(T_0 + T_1)$ of the layer. Starting from a slightly subcritical stable static state of heat conduction the temperature difference is increased by about $\Delta T \approx 0.1$ K in a period of typically 30 min. Thereby a weak convection of travelling waves is first stimulated, travelling randomly in one or the other direction. When the waves travel across the thermocouple in the cell centre, a periodic signal is recorded, whose amplitude is time modulated. This convection mode is commonly denoted as a modulated travelling wave (MTW). A typical record is shown in Fig. 3. The initially small fluctuation T' increases within 20 min from $T' = \pm 0.05$ K at $t = 0$ to $T' = \pm 0.5$ K at $t = 2.5 \times 10^3$ s with a period of oscillation $\tau = 37$ s.

The feature of a travelling wave is displayed in Fig. 4, where 14 interferograms taken at equal time intervals of $\Delta t = 10$ s are shown. Due to the slender geometry of the test cell and the quasi-steady heating, two-dimensional convection is nearly established in the test volume with the axes of the travelling convection rolls parallel to the shorter side of the cell. The pattern moves from the left to the right side as seen by the shift of the fringes with increasing time. The interferograms correspond to a time interval $1700 \text{ s} \leqslant t \leqslant 1830$ s of the temperature record in Fig. 3. The modulation of the intensity of the temperature perturbation due to convection can clearly be recognized from the number of concentric fringes which vary in the individual interferograms. More fringes indicate higher convection intensity in the travelling convection rolls. The period of oscillation of the travelling wave is $\tau = 37$ s. This value is obtained from the temperature record in Fig. 3 and also from the interferograms of Fig. 4.

2.2.2. *Finite amplitude initial perturbation.* If the initial temperature ramp leading to a transcritical state exceeds a certain threshold value a zone of intensive finite amplitude convection is induced at the ends of the test cells. It turns out that this zone of intensive convection improves significantly the overall heat transfer. Since the heat supply is limited by the coolant flux through the lower copper-block of the test apparatus the temperature difference in the central range of the test section is slightly reduced to a subcritical value. As a result a perturbation front moves from the ends of the test cell towards the centre. When this perturbation front moves across the thermocouple in the cell centre a monotonically amplified periodic temperature signal is recorded whose amplitude, after a short transition period, reaches a saturation value. The proceeding perturbation front is depicted by the set of the interferograms of Fig. 5. The interferograms are taken at time intervals $\Delta t = 8$ s. The front propagates at the low speed of $V = 1 \times 10^{-5}$ m s^{-1}.

The cellular fringe pattern indicates regular convection cells. In this particular case of strong initial perturbations the travelling waves propagate opposite to the perturbation front. Observations show that the front new convection rolls are repeatedly created which then move at a higher speed towards the cell end. The thermocouple records a period of oscillation of $\tau = 86$ s which is by a factor of 3 larger than the value at onset of the convection. A schematic streamline pattern as conjectured from the interferograms is added in Fig. 5.

Once the convection front reaches the opposite end of the test cell the temporal character of the travelling waves changes once more. The thermocouple record shows an increase of the amplitude by 25% and of the period of oscillation by about 400%. This effect is attributed to the interaction of the original wave and

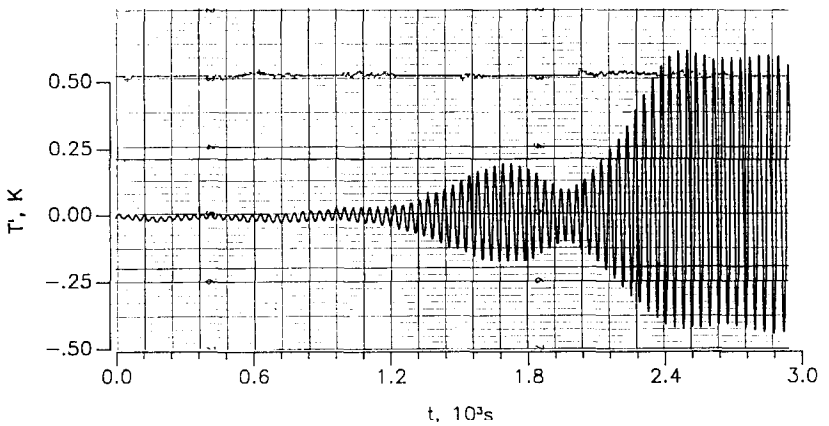

FIG. 3. Amplified local temperature fluctuations indicating the transition from a MTW- to a TW-mode, $C_0 = 15$ wt%, $\bar{T} = 10$°C.

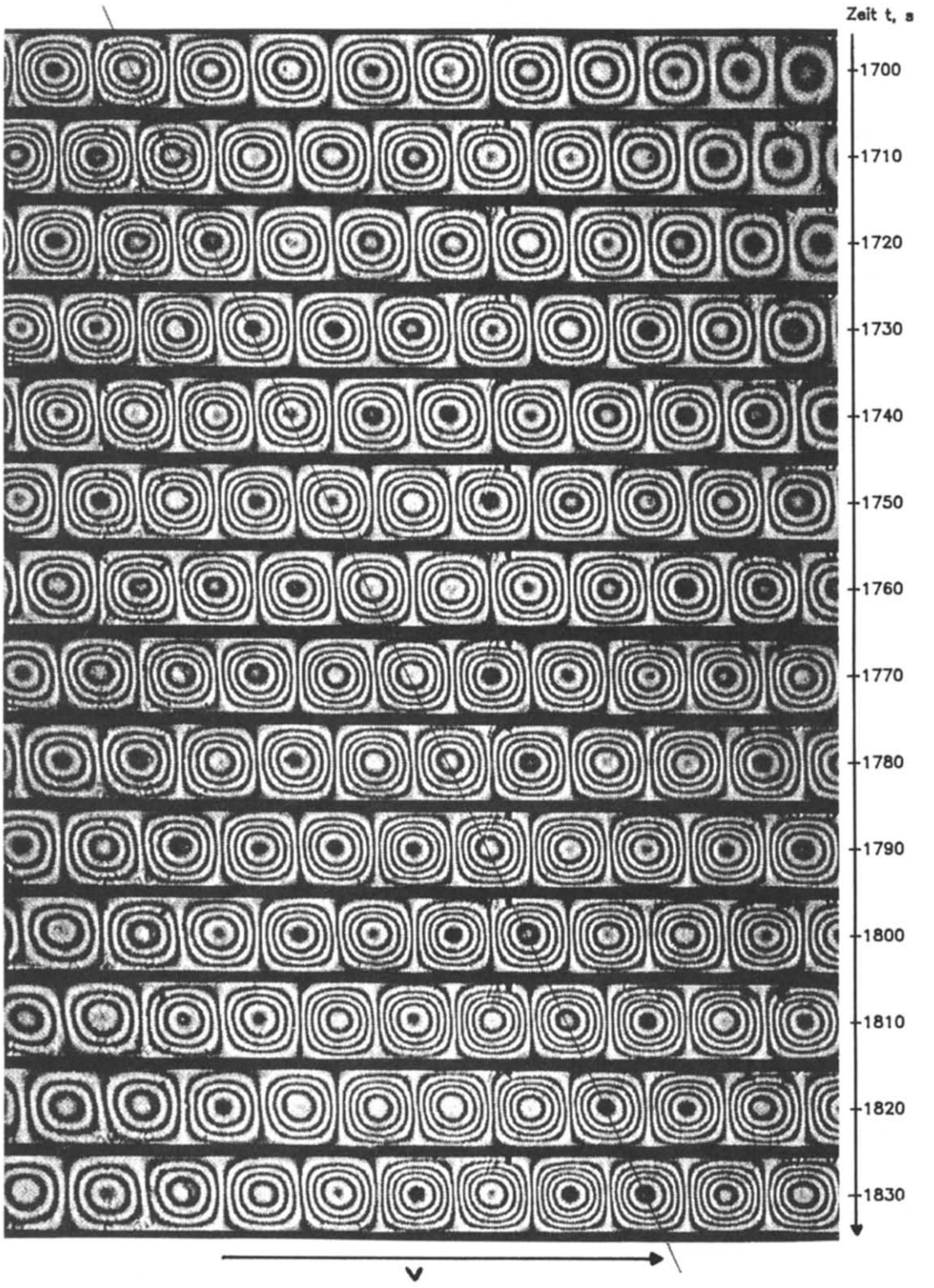

FIG. 4. Differential interferograms of a MTW at equal time intervals $\Delta t = 10$ s, $C_0 = 15$ wt% and $\bar{T} = 10$°C (see Fig. 3).

a reflected wave originating from the other end of the test cell. The time period for the transition in the temperature record is compatible with the propagation speed of the travelling waves obtained from interferograms and the dimensions of the test cell. The final state of the long period travelling waves is stable and persists for several days for fixed external temperature boundary conditions.

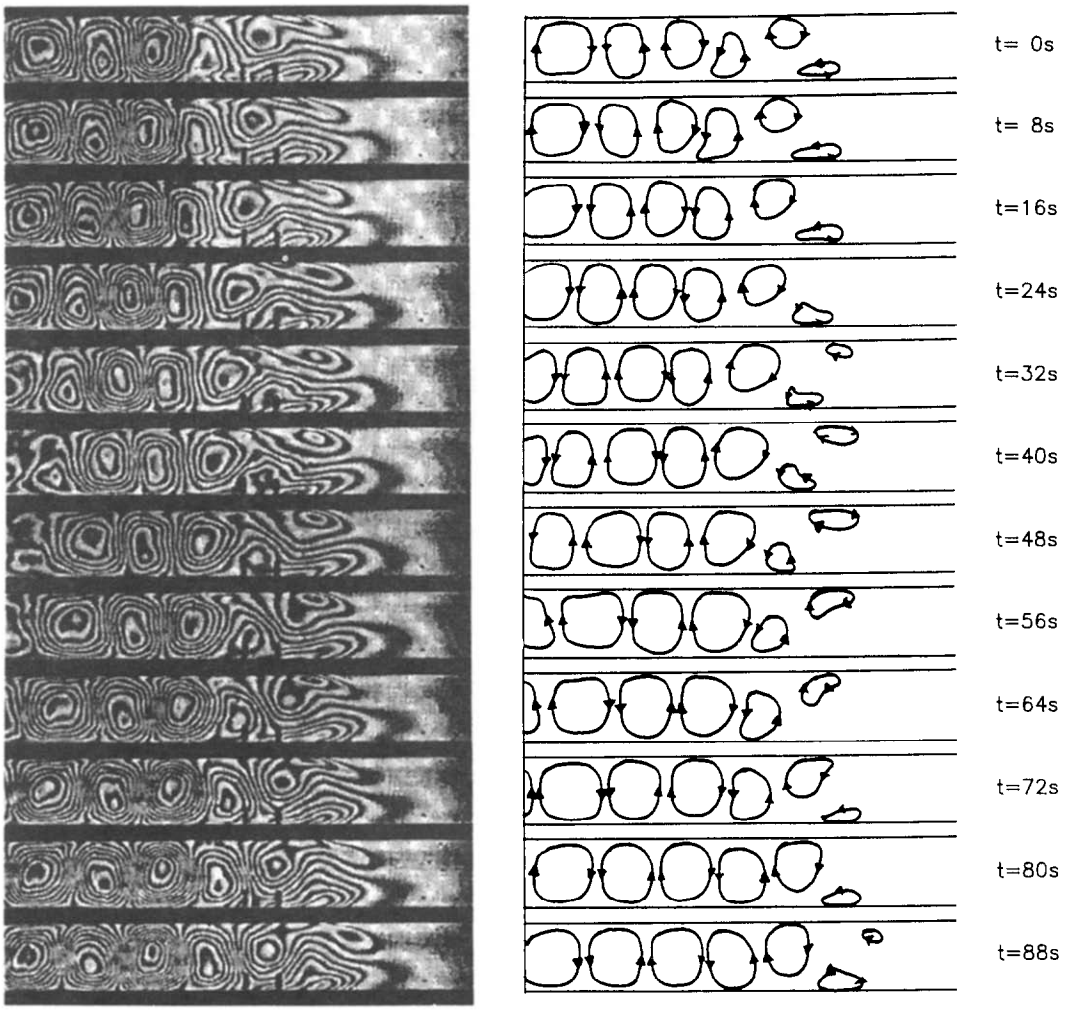

FIG. 5. Differential interferograms and streamline patterns (schematic) demonstrating a progressing perturbation front and waves travelling in opposite direction. Time intervals between interferogram Δt = 8 s, C_0 = 15 wt% and $\bar{T}$ = 10°C.

2.2.3. *Permanent travelling waves.* The permanent state of travelling waves in the test cell of finite length is investigated with regard to changing temperature differences ΔT across the liquid layer.

When ΔT is increased the period of oscillation increases continuously until finally, at a certain threshold temperature difference, a jump transition occurs to steady overturning convection which is, moreover, observed for even higher temperature differences. The measurements show that the oscillation frequencies depend linearly on the Rayleigh number in a range near the transition to steady overturning convection. A linear least square fit of the frequency data gives the relations $f = a - br$ with a = 16.5 (mHz), b = 9.8 (mHz) for C_0 = 8 wt% and a = 8.4 (mHz), b = 5.2 (mHz), for C_0 = 15 wt%, where r is the reduced Rayleigh number $r = R/R_c$. If ΔT is reduced, starting from steady state convection, travelling waves are observed down to a noticeably lower value ΔT compared to the one where steady convection is first seen for increasing ΔT. Thus, the transition from travelling waves to overturning convection and reverse shows a significant hysteresis. A similar phenomenon is observed for the onset of travelling wave motion from the static state. Decreasing ΔT across the layer, the travelling wave mode persists to significantly lower values of ΔT compared to its critical value for the onset of travelling wave motion.

The range of existence of permanent travelling waves is explored for two mixtures of ethyl alcohol and water with C_0 = 8 and 15 wt%. The experiments with these mixtures are carried out at mean temperatures $\bar{T}$ = 20 and 10°C respectively. The results are given in Figs. 6 and 7 in the form of graphs showing the oscillation period as a function of the normalized Rayleigh number $r = R/R_c$ where R_c = 1708 is the critical Rayleigh number for onset of convection in a single component liquid. Both mixtures show qualitatively the same behaviour. They differ, however, quantitatively in the measured periods and in the range where hysteretic behaviour is observed. This can be seen from Table 1 where the transitions

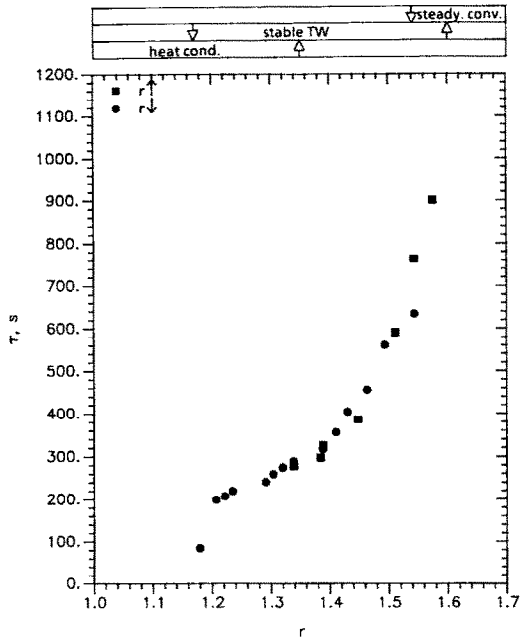

FIG. 6. Period of oscillation τ of the permanent TW-state as a function of the normalized Rayleigh number r, $C_0 = 8$ wt%, $\bar{T} = 20$°C.

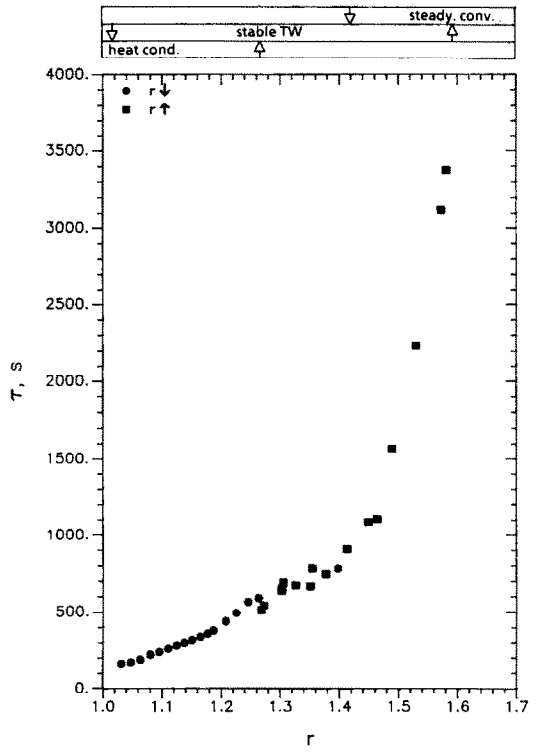

FIG. 7. Period of oscillation τ of the permanent TW-state as a function of the normalized Rayleigh number r, $C_0 = 15$ wt%, $\bar{T} = 10$°C.

Table 1. Critical Rayleigh numbers for the transitions heat conducting state-TW-state and TW-state-overturning convection state

	Transition	$C_0 = 8$ wt% $\bar{T} = 20$°C	$C_0 = 15$ wt% $\bar{T} = 10$°C
$r\uparrow$	Heat conduction → TW	1.35	1.27
	TW → Steady convection	1.60	1.59
$r\downarrow$	Steady convection → TW	1.54	1.42
	TW → Heat conduction	1.17	1.02

from the static state to the travelling wave and the steady state convection are listed.

For a particular permanent state of travelling waves the end effects in the test cell are visualized in Figs. 8 and 9. In Fig. 8 the temperature gradient field in the vicinity of the end of the test cell is demonstrated by a set of interferograms taken at time intervals of $\Delta t = 90$ s. The interferograms depict a situation where the waves move away from the cell end. The temperature difference is, in this case, $\Delta T = 7.0$ K and the initial concentration is $C_0 = 15$ wt%. From the fringe pattern it can be concluded that heat conduction prevails in a range $0 < L < 2h$ (the interferograms show equidistant and vertically oriented fringes). In a transition range $h < L \leqslant 10h$ the fringe increases continuously and the fringes become more and more contorted. The final permanent state indicated by concentric fringe patterns is established for $L > 10h$. It can be observed that the wave propagation velocity develops in this range from zero to its final value.

Figure 9 shows the situation of a wave moving towards the end wall of the test cell. From the set of interferograms a change in the intensity of the wave mode and the propagation speed cannot be identified in a region close to the end wall. However, a small decrease in the wavelength of about 10% can be measured in a region $L \leqslant 5h$.

2.2.4. *Steady state convection.* The experiments conducted at a mean temperature $\bar{T} = 10$°C and in a mixture of $C_0 = 15$ wt% show that stable travelling waves exist in a range of normalized Rayleigh numbers $1.02 \leqslant r \leqslant 1.59$. When the mean temperature of the liquid layer is reduced the range of existence of stable travelling waves becomes smaller and simultaneously the convection pattern gets less regular. For instance, convection rolls of different wavelength and different intensity occur. If the mean temperature $\bar{T}$ falls below the threshold value $\bar{T} \leqslant 5$°C permanent travelling waves are not observed. Thus, if in an experiment with $\bar{T} \leqslant 5$°C the temperature difference across the layer is increased beyond its critical value to $r = 1.89$, modulated travelling waves (MTW) are observed. This MTW state is amplified to a saturation amplitude. The saturated MTW propagates through the test cell usually starting at one end of the cell. Once this wave reaches the other end of the cell the velocity of the travelling wave slows down starting from this particular end. Finally an overturning steady state convection forms (see also Section 2.2.3).

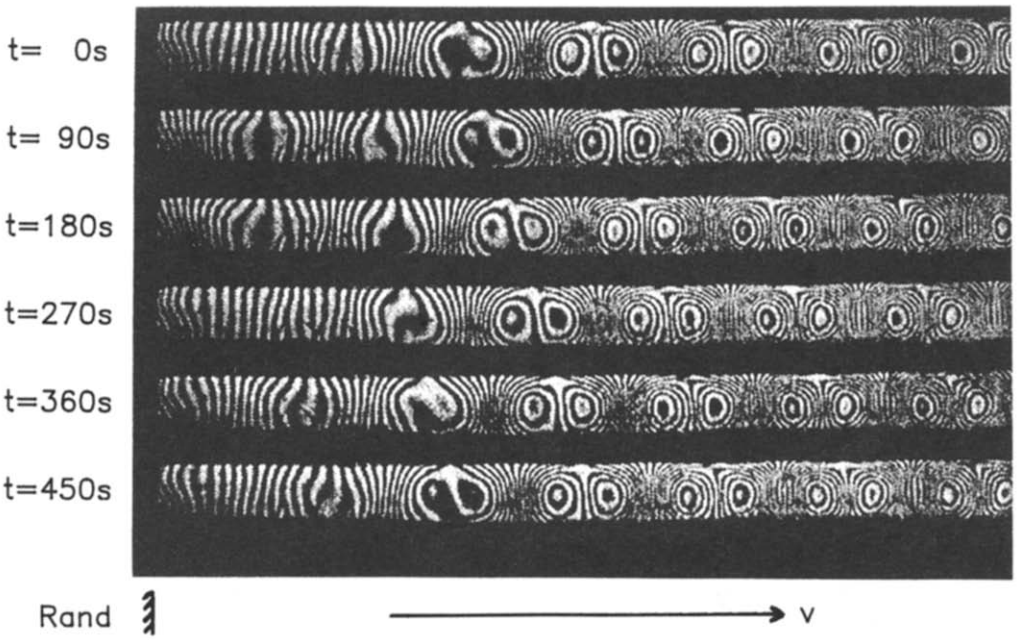

FIG. 8. Differential interferograms showing a TW-state near the end of the test cell. The TW moves toward the cell centre. Time interval between interferograms $\Delta t = 90$ s, $C_0 = 15$ wt% and $\bar{T} = 10$ °C.

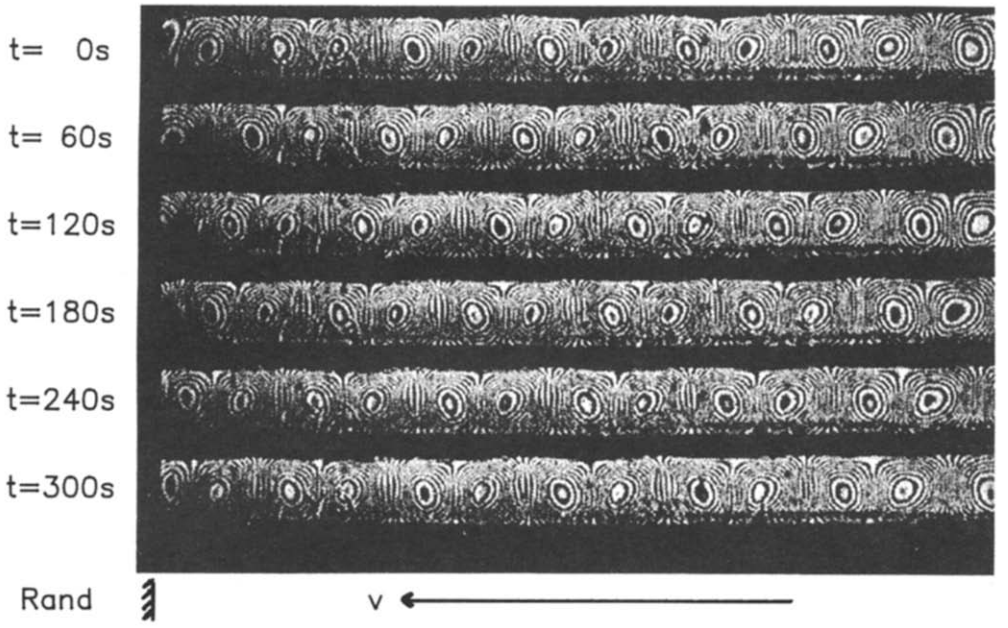

FIG. 9. Differential interferograms showing a TW-state near the end of the test cell. The TW moves toward the side wall, time interval between interferograms $\Delta t = 60$ s, $C_0 = 15$ wt% and $\bar{T} = 10$ °C.

3. DISCUSSION

The occurrence of a permanent oscillatory convection in the layer consisting of a mixture with negative Soret coefficient is the result of a double-diffusive mechanism, in which the temperature and concentration distribution have opposite stabilizing effects. Their spatial distributions diffuse with vastly different time scales τ_T and τ_D respectively. Since $\tau_T \ll \tau_D$, a warm fluid element that rises in the layer loses its characteristic temperature in time τ_T while its characteristic concentration remains practically unchanged. Thus, after equilibration of the temperature the parcel is too heavy compared to its environment, and falls back into a warmer layer. The descent of the parcel is on the longer time scale τ_c so

the density adjusts to the temperature distribution. The parcel becomes lighter and rises again due to thermal buoyancy. The cycle starts anew. The above physical arguments are reasonable to explain the occurrence of an oscillatory convection in which the velocity in the convection cell changes sign for each half period. The experiments show, however, that this oscillatory state, which can be considered a standing wave, is not realized as a permanent state, rather travelling roll patterns are observed.

The time and space dependent process in the layer can indeed be described mathematically as propagating waves of temperature, concentration and velocity. This has been done by, among others, Knobloch [18], Cross [19] and Linz *et al.* [20]. In their weakly nonlinear analysis Linz *et al.* [20] discuss solutions of travelling waves (TW), modulated travelling waves (MTW), standing waves (SW) and overturning steady convection (OSC). They find for travelling waves a phase shift between the concentration, the velocity and the temperature fields. The phase shift between the temperature and concentration wave gives rise to a horizontal pressure variation along streamlines of a convection cell. This horizontal pressure variation makes the convection cells move in the preferred direction. The phase shift vanishes between the temperature and concentration field for standing waves. As a result there exists a net flux of the lean component in travelling wave convection whereas the time average flux vanishes for standing waves. A rather general result for wave propagation in double diffusive systems has been obtained by Knobloch [18]. Applied to two component systems with Soret effect their analysis proves that near the critical Rayleigh number for onset of oscillatory convection the standing wave mode is unstable if a stable travelling wave mode bifurcates supercritically, and vice versa. If the bifurcation of the travelling wave occurs subcritically it is locally unstable and so is the related standing wave mode.

For our experiments we observe modulated travelling waves, travelling waves and overturning convection. Permanent standing waves do not occur for the realized experimental conditions. The hysteresis effect related to the transition from the static state to the travelling wave mode as well as the sensitivity to finite amplitude perturbations in our experiments suggest that we have a subcritical bifurcation of the travelling wave mode which is thus locally unstable according to theory. The instability of the small amplitude travelling wave may also be concluded from the long term growth of the state variables, e.g. $T'(t)$, until they settle down to a finite saturation value. This finite amplitude permanent travelling wave mode of the experiment is not described by the weakly nonlinear theory of Knobloch [18], Cross [19] or Linz *et al.* [20]. However, Bensimon *et al.* [23] have developed a nonlinear theory, which also describes the permanent travelling waves of finite amplitude and their transition to steady overturning convection.

Some features of the unstable modulated travelling waves of small amplitude are adequately described by the linear stability analysis.

Consider the configuration where the horizontal parallel plates of infinite horizontal extent are separated by a distance h. The lower plate has the fixed temperature $T = T_0$ while the upper plate has the fixed temperature $T = T_1$. The material between the plates is a two-component liquid. The material properties are constant. The lean component has diffusivity D and Soret coefficient So. The sign of So is defined as usual in the literature. In the case of $So > 0$ the more dense component diffuses toward the upper, colder boundary. The velocity is $v = (u, v, w)$.

The convection will be described using the Boussinesq equations. Therefore we have in the liquid (see ref. [16]),

$$\frac{\partial}{\partial t} v + v \cdot \nabla v = -\frac{1}{\rho_0} \nabla p + \nu \nabla^2 v + [\alpha(T - T_1) + \alpha'(C - C_0)] g \quad (1)$$

$$\nabla \cdot v = 0 \quad (2)$$

$$\frac{\partial}{\partial t} T + v \cdot \nabla T = \kappa \nabla^2 T \quad (3)$$

$$\frac{\partial}{\partial t} C + v \cdot \nabla C = -\nabla \cdot j \quad (4)$$

$$\rho = \rho_0 [1 - \alpha(T - T_1) - \alpha'(C - C_0)]. \quad (5)$$

Here ρ_0, C_0 are the mean density and mean mass fraction of the solute. The flux j, allowing for Soret diffusion, takes the form

$$j = -D[\nabla C - So\, C(1 - C) \nabla T]. \quad (6)$$

At the upper and lower boundary at $z = h$ and $z = 0$ the temperatures are fixed and the boundaries are rigid. Thus we have

$$T = T_1, \quad u = v = w = 0, \quad z = h$$

$$T = T_0, \quad u = v = w = 0, \quad z = 0. \quad (7)$$

At the rigid boundaries the concentration flux vanishes

$$j \cdot n = 0 \quad \text{at} \quad z = 0, h. \quad (8)$$

The equations (1)–(5) and the boundary conditions (6)–(8) can be transformed into a dimensionless form by introducing a set of non-dimensional numbers. We perturb the governing system (1)–(5) about the static basic state and introduce normal modes for each disturbance quantity.

We get a boundary-eigenvalue problem which is solved numerically by means of a shooting method. For this the SUPORE-CODE of Scott and Watts [24] is used. A detailed description of the procedure and more numerical results are given by Zimmermann [17] and Zimmermann *et al.* [25].

In Table 2 a comparison between measured and calculated values for the critical Rayleigh number and the period of oscillation is presented for mixtures of

Table 2. Critical Rayleigh numbers and dimensionless periods of oscillation, comparison between theory and experiment

	Concentration / temperature	8 wt% 20°C	15 wt% 10°C	15 wt% 5°C
$R_c^{(o)}$	Experiment	2306	2166	3320
	SUPORE	2601	2673	2940
τ/τ_T	Experiment	0.507	0.401	0.362
	SUPORE	0.442	0.399	0.376

$C_0 = 8$ and 15 wt% ethyl alcohol and water and for different mean temperatures of the liquid layer. The differences between the calculated and the measured quantities in particular for the case $\bar{T} = 10°C$ are mainly attributed to uncertainties in the Soret coefficient. The value used in our evaluation is taken from Kolodner *et al.* [21]. Generally the values found in the literature for S may differ up to 25%. Other sources for the discrepancy may be the effectively nonlinear density temperature relation in mixtures and the finite extent of the test volume. Both effects are stabilizing and should give rise to higher critical values for $R_c^{(o)}$ and $\omega_c^{(o)}$.

The progression of a perturbation front into an unstable static state with waves travelling in opposite directions, as demonstrated by Fig. 5, can be compared with observations by Kolodner [26], who reports an experiment in which slow travelling rolls exist in a confined region of an arbitrary length in a rectangular cell separated from the rest by a front that may slowly move or be motionless. A model to describe this phenomenon qualitatively has been proposed by Bensimon *et al.* [27]. The model is based on two coupled, generalized Landau–Ginsburg equations. The model contributes physical explanations for the observed phenomena, but does not describe them quantitatively.

The influence of a finite geometry of the test cell on wave systems has been investigated by Moses *et al.* [28], Surko *et al.* [29] and Ahlers *et al.* [10]. Cross [19, 30] investigates this question theoretically. He studies the reflection of waves at the vertical boundaries of test volumes using Landau–Ginsburg type amplitude equations. If the group velocity of the wave system is small the weakly nonlinear interaction of right and left side propagating waves results in a travelling wave state of preferred direction and uniform intensity in the major part of a horizontally elongated test cell. Only in the vicinity of the confirming side walls does the interaction of the incoming and reflected wave lead to partial annihilation or the formation of a stationary convection depending on the direction of propagation of the wave in the cell centre. Cross finds that the travelling wave is fully developed at a distance $L \approx 10h$ from the side wall where it originates; at the opposite side the impact of the wave on the vertical boundary is noticed at a distance of $L \approx 5h$. These predictions are qualitatively confirmed by our observations as demonstrated by Figs. 8 and 9.

The measured oscillation period of the permanent travelling wave state (see Section 2.2.3) does not scale properly with either the thermal or the mass diffusion time scale h^2/κ and h^2/D respectively. This seems plausible since this finite amplitude wave state is generally not near the bifurcation point for the onset of oscillatory convection. Observations of tracer particles in the convective flow by means of a stereomicroscope, indicate that the turn around time is typically of the order $\tau_t \approx 100$ s. The transport of the lean component within a moving convection roll (i.e. a travelling wave) can, to a good approximation, be described by the transport along closed streamlines in a coordinate system moving with the phase velocity of the wave. According to Rhines and Young [31] this process can be described by the following transport equation

$$\frac{\partial C}{\partial t} + U\frac{\partial C}{\partial s} = D\nabla^2 C \tag{9}$$

where U is the transport velocity along a particular streamline, s is the coordinate along the streamline and ∇^2 is the two-dimensional Laplace operator in a corresponding orthogonal coordinate system. They obtain for a simple shear flow solution of the form

$$C(t) = C_0 \exp\left|-\left(\frac{t}{\tau_D}\right)-\left(\frac{t}{\tau_{mix}}\right)^3\right| \cos k(s-ayt) \tag{10}$$

where $\tau_D = h^2/D$ and $\tau_{mix} = (U^2 D/h^4)^{1/3}$. Introducing a Peclet number $Pe = (U \cdot h/D)$ we obtain $\tau_{mix} \sim Pe^{1/3}$. The form of the solution, equation (9), indicates that for large times the time scale τ_{mix} determines the diffusion process in the vicinity of streamlines and thus the equalization of the concentration field within a moving convection cell.

Since the local Peclet number Pe and the turnaround time are directly related to the intensity of the convective flow and thus to the excess Rayleigh number $\Delta R = R - R_c$, it is plausible that the transition from the travelling wave mode to steady overturning convection (see Section 2.2.3) is due to an equalization of the concentration field by a transport-enhanced diffusion according to equation (9). We conjecture that τ_{mix} is the proper time scale for the period of oscillation for the observed permanent travelling waves. Assuming the observed turn around time $\tau_t \approx 10^2$ s and the dimension $h = 3$ mm of our test volume and a typical diffusion coefficient $D \approx 4 \times 10^{-10}$ m^2 s^{-1} we obtain a Peclet number $Pe \approx 90$ and the corresponding mixing time scale $\tau_{mix} \approx 450$ s. This value is of the order of the observed oscillation periods listed in Figs. 6 and 7.

The temperature records from the thermocouple in

our test section show that the generally periodic signal is intermittently disturbed by irregularities. They occur particularly for the shorter periods of oscillation and in the lower range of Rayleigh numbers, while at higher Rayleigh numbers and for longer periods such irregularities are not observed. Other authors refer to a similar observation as chaotic behaviour which also involves pattern irregularities (e.g. see ref. [4]). Our observations show that the temporal irregularities are related to irregularities in the wave number spectrum of the travelling waves. A complete theoretical model to explain this spatio-temporal feature is not available, to our knowledge. A linear relationship between the frequency and the Rayleigh number (see Section 2.2.3) as well as the hysteretic behaviour of the transition from the travelling wave mode to steady overturning convection has been observed. It is also predicted in the theoretical works of Knobloch [18], and by the numerical simulations of Deane *et al.* [32].

Unexpectedly permanent travelling waves are not observed in ethyl alcohol mixtures if the average layer temperature is decreased to values that come close to the solidification temperature of the mixture, e.g. $\bar{T} < 5°C$ for a mixture of $C_0 = 15$ wt%. Instead of a travelling wave mode a steady three-dimensional convection pattern develops. This effect is felt even for higher mean temperatures since the range, where permanent travelling waves are observed, shrinks when the average temperature is decreased. It is conjectured, that this effect is due to the increasing nonlinearity of the density–temperature relation for the mixture and is not related to the temperature dependence of the Soret coefficient (see Kolodner *et al.* [26]). A theoretical analysis of the situation, i.e. the effect of non-Boussinesq properties on wave propagation in binary mixtures, is to date, not available.

4. SUMMARY

We have performed experiments of Benard convection in a binary mixture with Soret effect. We use a differential interferometer to visualize the convection patterns by interferograms and record the temperature history at a particular location inside the liquid layer. We observe an amplified travelling roll pattern of transient character whose intensity is modulated in space and time as long as its value is below a certain threshold. This travelling roll pattern starts at the shorter sidewalls. Once the value is exceeded the amplitudes of the convection saturate and a convection front propagates into the test cell. This transient state ends up in a stable, nonlinear travelling wave state. There is a transition from this state of travelling waves to steady overturning convection for an even higher threshold Rayleigh number. This transition, as well as the transition from the static state of heat conduction to the state of travelling wave convection, show strong hysteresis effects. Permanent travelling waves are suppressed for low mean temperatures of the liquid layer. Instead a quasi-steady three-dimensional irregular convection pattern is identified. It is conjectured that this phenomenon is due to the actual nonlinear density–temperature relation of the binary mixture at temperatures close to the liquidus temperature. The outlined observations are in agreement with results reported in the literature.

REFERENCES

1. D. R. Caldwell, Thermosolutal convection in a solution with large negative Soret coefficient, *J. Fluid Mech.* **74,** 129–142 (1976).
2. D. T. Hurle and E. Jakeman, Soret-driven thermosolutal convection, *J. Fluid Mech.* **47,** 667–687 (1971).
3. J. K. Platten and G. Chavepeyer, Oscillatory motion in Benard cell due to Soret effect, *J. Fluid Mech.* **60,** 305–319 (1973).
4. R. W. Walden, P. Kolodner, A. Passner and C. M. Surko, Travelling waves and chaos in convection in binary fluid mixtures, *Phys. Rev. Lett.* **55,** 496–499 (1985).
5. P. Kolodner, A. Passner, C. M. Surko and R. W. Walden, Onset of oscillatory convection in a binary fluid mixture, *Phys. Rev. Lett.* **56,** 2621–2624 (1986).
6. P. Kolodner, A. Passner, H. L. Williams and C. M. Surko, The transition to finite-amplitude travelling-wave convection in binary fluid mixtures, *Nuclear Phys. B* (Proc. Suppl.) **2,** 97–108 (1987).
7. C. M. Surko and P. Kolodner, Oscillatory travelling-wave convection in a finite container, *Phys. Rev. Lett.* **58,** 2055–2058 (1987).
8. E. Moses and V. Steinberg, Mass transfer in propagating patterns of convection, *Phys. Rev. Lett.* **60,** 2030–2033 (1988).
9. V. Steinberg, E. Moses and J. Fineberg, Spatio-temporal complexity at the onset of convection in a binary fluid, *Nuclear Phys. B* (Proc. Suppl.) **2,** 109–124 (1987).
10. G. Ahlers, D. S. Cannell and R. Heinrichs, Convection in a binary mixture, *Nuclear Phys. B* (Proc. Suppl.) **2,** 77–86 (1987).
11. J. Fineberg, E. Moses and V. Steinberg, Spatially and temporally modulated travelling-wave pattern in convecting binary mixtures, *Phys. Rev. Lett.* **61,** 838–841 (1988).
12. J. Fineberg, E. Moses and V. Steinberg, Nonlinear pattern and wave-number selection on convecting binary mixtures, *Phys. Rev.* **A38,** 4939–4942 (1988).
13. D. Bensimon, A. Pumir and B. J. Shraiman, *J. Physique* **50,** 3089 (1989).
14. R. S. Schechter, I. Prigogine and J. R. Hamm, Thermal diffusion and convective stability, *Physics Fluids* **15,** 379–386 (1972).
15. J. C. Legros, J. K. Platten and P. G. Poty, Stability of a two-component fluid layer heated from below, *Physics Fluids* **15,** 1383–1390 (1972).
16. D. P. Chock and Chin-Hsiu Li, Direct integration method applied to Soret driven instability, *Physics Fluids* **18,** 1401–1406 (1975).
17. G. Zimmermann, Benard-Konvektion in binären Flüssigkeitsmischungen mit Thermodiffusion, Dissertation Universität Karlsruhe und KfK 4683 (1990).
18. E. Knobloch, Oscillatory convection in binary mixtures, *Phys. Rev.* **A34,** 1538–1549 (1986).
19. M. C. Cross, An eight-mode Lorenz-model of travelling waves in a binary fluid convection, *Phys. Lett.* **A119,** 21–24 (1986).
20. S. J. Linz, M. Lücke, H. W. Müller and J. Niederländer, Convection in binary fluid mixtures: travelling waves and lateral currents, *Phys. Rev.* **A38,** 5727–5741 (1988).
21. P. Kolodner, H. Williams and C. Moe, Optical measure-

ment of the Sorét coefficient of ethanol/water solutions, *J. Chem. Phys.* **88,** 6512–6524 (1988).
22. K. Bühler, K. R. Kirchartz and J. Srulijes, Anwendung der Differentialinterferometrie bei thermischen Konvektionsströmingen. In *Applied Fluid Mechanics* (Edited by H. Oertel, Jr.), S.54–69 (1978).
23. D. Bensimon, P. Kolodner, C. M. Surko, H. Williams and V. Croquette, Competing and coexisting dynamical states of travelling-wave convection in an annulus, *J. Fluid Mech.* **217,** 441–467 (1990).
24. M. R. Scott and H. A. Watts, Subroutine SUPORE, Applied Mathematics Division 2623, Sandia Laboratories, Rep. SAND 75-0198, Albuquerque, New Mexico (1975).
25. G. Zimmermann, U. Müller and S. H. Davis, Bénard convection in binary mixtures with Soret effect and solidification, *J. Fluid Mech.* in press (1992).
26. P. Kolodner, Neutrally stable fronts of slow convective travelling waves, *Phys. Rev.* **A42,** 2475–2478 (1990).
27. D. Bensimon, B. J. Shraiman and V. Croquette, Nonadiabatic effects in convection, *Phys. Rev.* **A38,** 5461–5464 (1988).
28. E. Moses, J. Fineberg and V. Steinberg, Multistability and confined travelling-wave patterns in a convecting binary mixture, *Phys. Rev.* **A35,** 2757–2760 (1987).
29. C. M. Surko, P. Kolodner, A. Passner and R. W. Walden, Finite-amplitude travelling-wave convection in binary fluid mixtures, *Physica* **23D,** 220–229 (1986).
30. M. C. Cross, Structure of nonlinear travelling-wave states in finite geometries, *Phys. Rev.* **A38,** 3593–3600 (1988).
31. P. B. Rhines and W. R. Young, How rapidly is a passive scalar mixed within closed streamlines? *J. Fluid Mech.* **133,** 133–145 (1983).
32. A. E. Deane, E. Knobloch and J. Toomre, Travelling waves and chaos in the thermosolutal convection, *Phys. Rev.* **A36,** 2862–2869 (1987).

CONVECTION DE BENARD DANS UN SYSTEME BINAIRE AVEC EFFET SORET

Résumé—Le comportement spatial et temporel de la convection de Rayleigh–Bénard dans un système à deux composants avec effet Soret est étudié en employant l'interférométrie différentielle en combinaison avec des enregistrements de température locale dans la couche liquide. Des configurations à tourbillons ayant un caractère variable ou permanent sont observées. Les fréquences associées avec les ondes progressives sont déterminées et comparées avec les prédictions de l'analyse de stabilité linéaire et interprétées en fonction du transport solutal et du mélange le long des lignes de courant. Une constatation imprévue est que le domaine d'apparition de l'état permanent des ondes progressives se rétrécit quand les effets non Boussinesq dominent.

BENARD-KONVEKTION IN EINEM BINÄREN SYSTEM MIT SORET-EFFEKT

Zusammenfassung—Das räumliche und zeitliche Verhalten der Rayleigh–Benard Konvektion in einem binären System mit Soret-Effekt wird mit Hilfe eines Differentialinterferometers und lokaler Temperaturmessung in der Flüssigkeitsschicht untersucht. Dabei werden Muster transienter und stabiler Wanderwellenzustände sowie stationäre Konvektion gefunden. Die Frequenzen der Wanderwellen werden ermittelt und mit den Ergebnissen der linearen Stabilitätsanalyse verglichen und auf der Basis von Stofftransport zwischen den Konvektionsrollen interpretiert. Ein unerwartetes Ergebnis ist, daß der Existenzbereich der stabilen Wanderwellen mit zunehmendem nicht-Boussinesq'schen Einfluß schrumpft.

КОНВЕКЦИЯ БЕНАРА В ДВУХКОМПОНЕНТНОЙ СИСТЕМЕ ПРИ НАЛИЧИИ ЭФФЕКТА СОРЭ

Аннотация—С использованием дифференциальной интерферометрии в комбинации с регистрацией локальной температуры в слое жидкости исследуются пространственные и временные характеристики конвекции Рэлея – Бенара в двухкомпонентной системе при наличии эффекта Сорэ. Проводятся наблюдения структур валов нестационарного и устойчивого характера, а также установившейся валообразной конвекции. Определяются частоты, связанные с бегущими волнами; полученные результаты сравниваются с данными линейного анализа устойчивости и выражаются через характеристики переноса и смешения растворенного вещества вдоль линий тока. Найдено, что вопреки ожиданию область существования устойчивого состояния бегущих волн сокращается при доминировании эффектов, не описываемых аппроксимацией Буссинекса.